A Study on the Microstructure Development in Laser-Cladded Tantalum Layers

Kang Yuan[1,2,3] · Xiaoxiao Pang[1,2,3] · Ziqiang Pi[1,2,3] · Xiaoliang Lu[1,2,3]

Abstract In this study, the microstructure development of a laser-cladded tantalum (Ta) layer formed on an iron (Fe) substrate was mainly analyzed. The results showed that typical dendritic crystalline structures were formed in the Ta layer. Fe was detected in the Ta layer, indicating that the upward diffusion of Fe from the substrate occurred. By applying thermodynamic and kinetic calculations, the microstructure development observed in the experiment can be well understood. In the fully molten zones, typical eutectic structure was formed containing BCC-Ta dendrite and MU-TaFe inter-dendrite. While in the partially molten zone away from the laser heating, spherical Ta particle morphology was kept without dendritic structure. To achieve purer Ta layers or coatings by minimizing the effect of the upward diffusion of substrate elements, a high-melting-point tungsten substrate was used in both laser cladding and plasma spraying processes.

✉ Kang Yuan
bityuankang@126.com

1 BGRIMM Technology Group, Beijing 100160, China

2 BGRIMM Advanced Materials Science and Technology Co., Ltd, Beijing 102206, China

3 Beijing Engineering Technology Research Center of Surface Strengthening and Repairing of Industry Parts, Beijing 102206, China

Introduction

Tantalum (Ta) is an important refractory element in chemical, medical care, and electronic industries (Ref 1-3). When making coatings or 3D-printing structures, spherical Ta powders are required to have a good flowability and apparent density. Inductive plasma-sphero technique has been widely used to make the spherical powders by using commercial equipments (Ref 4-8). Laser cladding is an important coating technique with high manufacture efficiency and low-cost (Ref 9-12). Due to its high production rate, the laser cladding technique can be used to quickly make thick coatings, for example, rotating sputtering targets.

Some researchers studied the cladding behavior of Ta. Yang et al. made a 2.5 mm thick tantalum layer by using laser cladding technique to improve the resistance of a titanium substrate against inorganic acid corrosion (Ref 13). Their results indicated that the main phase of the Ta coating was a body-centered cubic phase, i.e., BCC-Ta, and the coating showed higher hardness and better corrosion resistance than the substrate. JP Kusinski et al. studied the microstructure and properties of Ta alloyed coatings, and found that the coatings showed high chemical homogeneity made by laser cladding (Ref 14). However, as Ta has a high melting point, usually higher laser energy should be used which, however, can cause larger melting pool and stronger upward diffusion of the substrate elements. The proper

selection of the cladding process parameters permitted to get coatings with low dilution of the base material. At present, the research on such topic is rare in the literature.

In this project, thick Ta layers were made by laser cladding technique on an iron substrate to study the possibility to make rotating sputtering targets. The microstructure development in a 5 µm-thick Ta layer was investigated with analyses of phase constitution using thermodynamic simulations. To get purer Ta layers, tungsten substrates and a plasma spraying technique were also tried to decrease the upward diffusion rate of substrate elements.
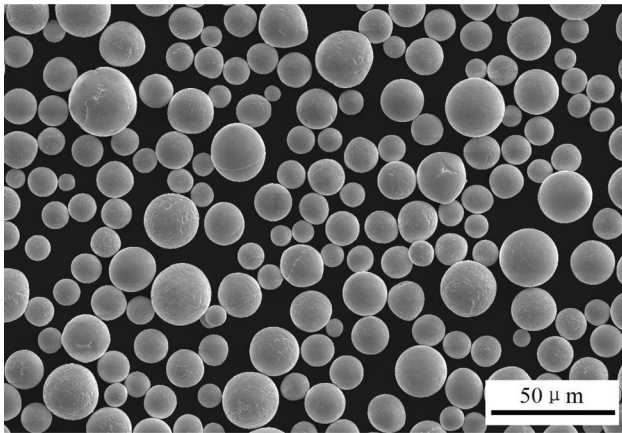
Experimentals

In this study, spherical Ta powders were made in BGRIMM technology group by using inductive plasma-sphero technique (TEKNA, Canada). The morphology of the spherical Ta powders is shown in Fig. 1. The size of the powders was between 5 and 40 µm. MF-LC2000 laser cladding system was used to make Ta layer on an iron substrate. The laser energy was set at 3.8 kW and the laser size was about 3.18 mm. In the laser cladding process, the powders were sent into high-energy laser zone laterally and were melted at the surface of the substrate. The powder feeding rate was ~ 70 g/min, the relative surface speed was 8.3 mm/s, and the working distance was 20 mm. After 9 cladding tracks, Ta layer with about 5 mm thickness was obtained. Such thick Ta layer was made aimed at studying the possibility of the coating techniques to produce rotating Ta sputtering targets which are usually within 3 to 20 mm thickness. The Ta powders were also used to make Ta coating on tungsten substrate by applying low-pressure plasma spray technology (LPPS-TF system, Oerikon Metco) with plasma power 105 kW, spraying distance 400 mm, powder feeding rate ~ 55 g/min, substrate rotating rate of ~ 150 rpm, relative surface speed of ~ 2 m/s and pressure below 100 mbar. The LPPS technique made ~ 0.7 mm thick coating by 1200 passes.

After the cladding or spraying process, the samples of Ta layers/coatings were cut, mounted and polished to study the microstructure. The microstructure of the materials was analyzed in a scanning electron microscope (SEM) (SU5000, Hitachi, Japan). The composition of different characterized zones in the material was detected by using XFlash 6130 energy dispersive microscope (EDS) (BRUKER).

Fig. 1 Morphology of pure Ta powder made by induced plasma sphero technique

Fig. 2 (a) Cross section of Ta-cladded layer showing Ta/(Ta + Fe) composition distribution, (b) composition profile along the laser center line
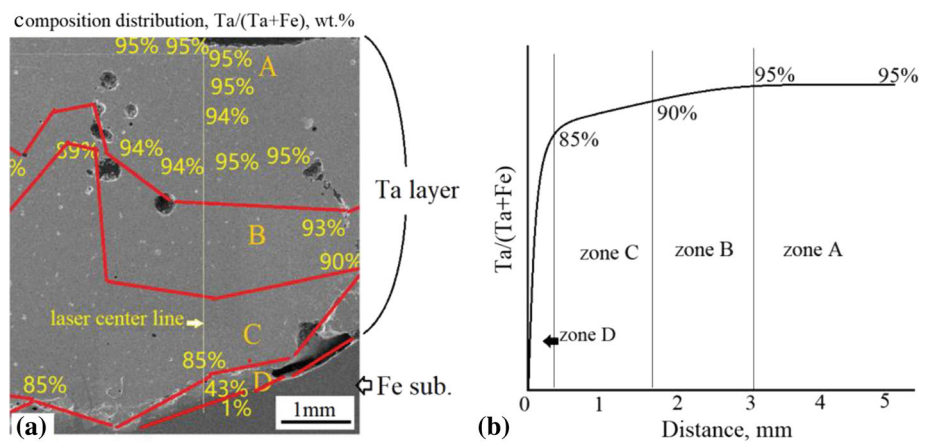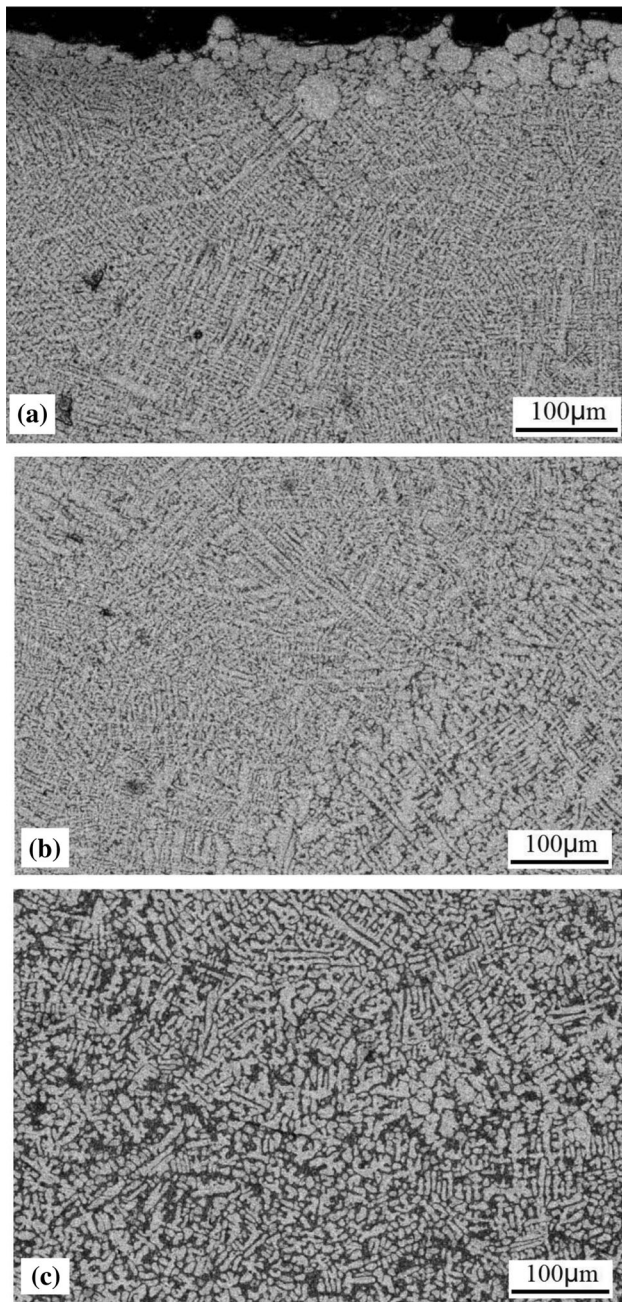
Fig. 3 Microstructure in different zones of Ta layer along the laser center line, (a) zone A, (b) zone B, (c) zone C

ThermoCalc software (ThermoCalc Software AB, Sweden) was used to simulate the phase constitution at different Ta-Fe compositions. Phase diagram of Ta-Fe for temperature range between 500 and 3500 °C was calculated. A commercial database, TCFE9, was applied in the thermodynamic simulations. To simulate elemental diffusion behavior in some characteristic zones, a "Ta core-Fe shell" model was built by applying DICTRA modulus in

the ThermoCalc software additionally using database of MOBFE6. Although the tool of ThermoCalc was generally used for equilibrium calculations, it can also help researchers to better understand the mechanism of the microstructure development in some non-equilibrium processes. In this study, the application of the Ta-Fe phase diagram indeed played such role.

Results and Analyses

Laser-Cladded Ta on Iron Substrate

Figure 2(a) shows the cross section of the Ta layer made by the laser cladding technique. Some casting pores were formed in the layer. The composition of Ta and Fe in different areas of the layer was measured by EDS. According to the results of the composition distribution, the layer was divided into four zones in the depth direction, i.e., zone A (Ta ≥ 95%), zone B (Ta 90-95%), zone C (Ta 85-90%) and zone D (Ta < 85%). The thickness of the A, B, C zones was around 1-2 mm, while zone D had a very small thickness. According to the composition profile along the laser center line (Fig. 2b), the upward diffusion of Fe from the substrate to the Ta layer occurred. As Ta had a much higher melting point ($\sim$ 3000 °C) than Fe ($\sim$ 1540 °C), the diffusion mobility of Fe was very high during the melting process of Ta in the cladding process. In zone D nearest to the Fe substrate which was the original melting pool, strong Fe diffusion took place. In zone about 2 mm away from the substrate (zone C), 10% Fe can be detected. Even up to $\sim$ 5 mm distance above the substrate, there was still about 5% Fe existing in the Ta layer. Therefore, the Ta layer became a Ta-Fe alloying layer.

Microstructure along the center line of the cladded layer was varied for the different zones. Typical dendritic crystalline (eutectic) structures were formed in those zones. In zone A (Fig. 3a), some unmelted Ta particles were also found at the surface. Comparing with the interdendritic phase, the dendritic phase were brighter in the backscattered electron images; the EDS measurement further detected higher Ta content in the dendrites (nearly 100% of Ta). In the zones closer to the substrate (Fig. 3b, c), the fraction of the dendrites decreased with the increase in Fe content. The size of the dendrites was also coarser near the substrate derived from the longer heated time of those zones during the laser cladding process.

The difference of the dendritic and inter-dendritic phase fraction in different zones can be explained in the Ta-Fe phase diagram. Figure 4 gives the phase diagram calculated by Thermo-Calc software. In zone A (Fig. 5a), according to the phase diagram, the dendrite "1" (EDS composition: 98%Ta2%Fe, Table 1) was probably BCC-Ta

Fig. 4 Phase diagram of Ta-Fe calculated by Thermo-Calc software using TCFE9 database
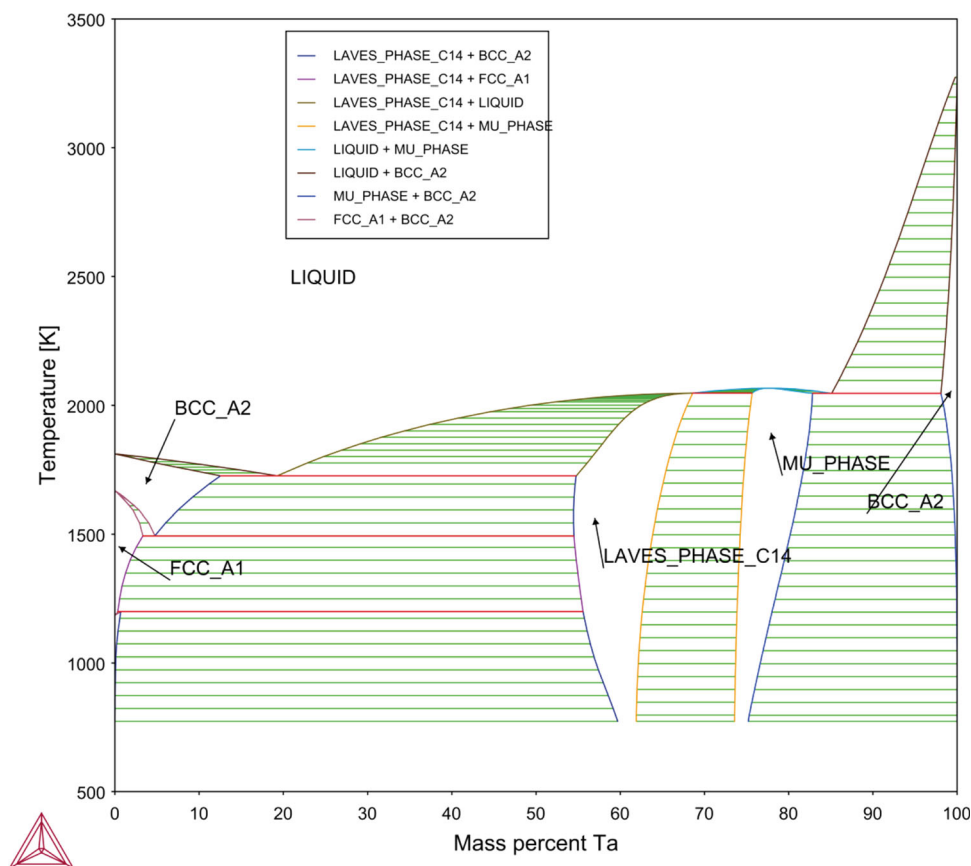
(Ta rich body-center cubic phase) phase while the interdendritic phase "2" (83%Ta17%Fe) could be MU-TaFe (MU is a topologically closely packed (TCP) phase). Such dendritic microstructure was formed due to the solidification of the Ta-Fe molten liquid (95%Ta5%Fe), which can be described by the blue line in the phase diagram (Fig. 5a). Figure 5(b) and (c) are fetched from zone D. Zone D was formed as an original molten pool at the beginning of the growth of the Ta-cladded layer. Because of higher Fe concentration, the microstructure in Fig. 5(b) (∼ 15% Fe) contained more MU phase than that in zone A (∼ 5% Fe, Fig. 5a). In the area given in Fig. 5(c), where ∼ 60% Fe were detected, more complicate phases were formed including BCC-Ta, BCC-Fe (Fe rich body-center cubic phase), and Laves-TaFe (Ta and Fe contained Laves phase, Laves also belongs to TCP phases).

As shown above, Ta powders were fully molten (FM) in the laser melting zones. However, in the cladding process, some Ta powders would also fly away from the laser beam to form partially molten (PM) zone, as shown in Fig. 6(a). Some defects such as pores or cracks can be formed at the interface between the FM and PM zones. Figure 6(b) gives a typical microstructure formed in the PM zone. The results showed that the composition of the PM zone

(95%Ta5%Fe) was similar to the FM zone A. But the BCC-Ta phases were presented in a spherical structure, indicating that the Ta powders here were not fully molten due to lower heating temperature away from the laser center. The formation of the two phases in this zone ("1" BCC-Ta, "2" MU-TaFe, Table 1) could be explained by the results in the phase diagram shown by the red line which started not from pure liquid but from the liquid + BCC-Ta phases.

In some areas such as at the corner of the PM zones, some solid diffusion microstructure was observed as shown in Fig. 7(a). Between the BCC-Ta core ("1", 98%Ta2%Fe) and the BCC-Fe shell ("3", 1%Ta99%Fe), there formed another phase containing both Ta and Fe ("2"). According to its EDS composition (54%Ta46%Fe), such interdiffusion-induced phase may be Laves-TaFe. To further understand the elemental interdiffusion behavior between the Ta powder (as a core) and the Fe shell, a core–shell spherical model was built in the DICTRA modulus. As shown in Fig. 7(b), the spherical model was built composed of a Ta core with radius of 17 μm and a Fe shell with thickness of 8 μm. A homogenization function, namely rule of mixture (upper Wiener bound), was used to control the diffusivity of the elements in the model. The real
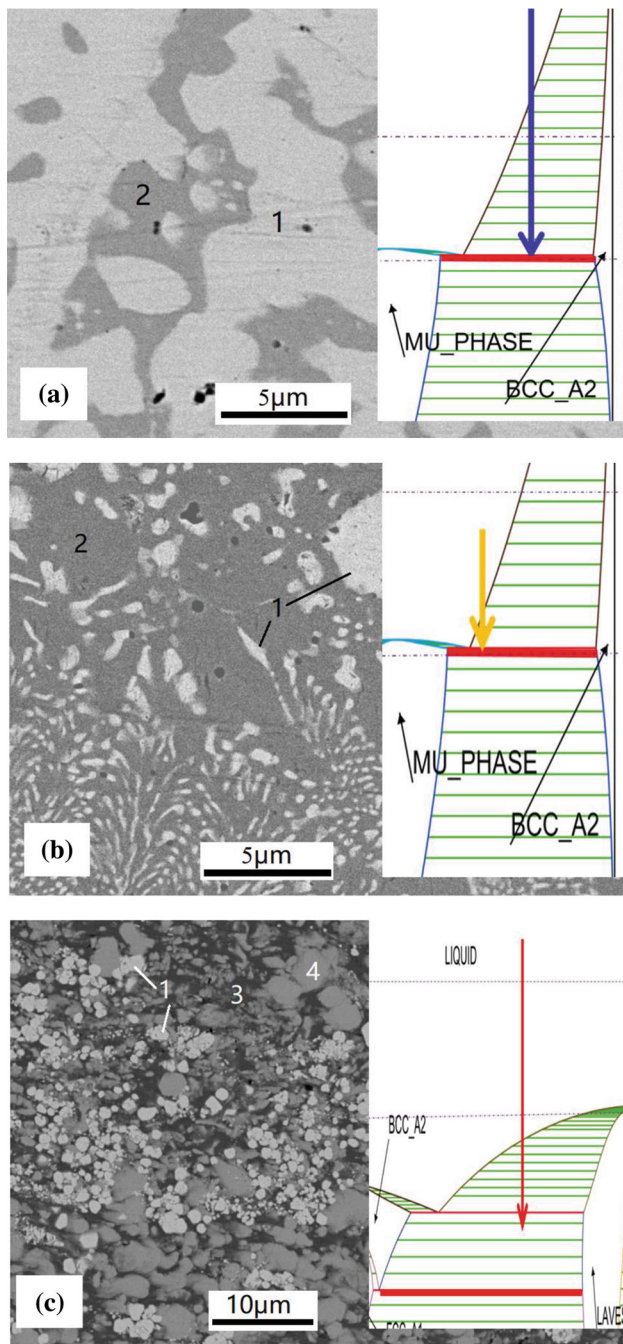
Fig. 5 Microstructure in different zones and their corresponding phase diagram, (a) zone A, (b) and (c) zone D

Table 1 EDS composition of phases (wt.%)

Characterized phase in figures	EDS composition	Possible phase according to phase diagram
"1" in Fig. 5(a)	98%Ta2%Fe	BCC-Ta[a]
"2" in Fig. 5(a)	83%Ta17%Fe	MU-TaFe[b]
"1" in Fig. 5(b)	96%Ta4%Fe	BCC-Ta
"2" in Fig. 5(b)	79%Ta21Fe	MU-TaFe
"1" in Fig. 5(c)	93%Ta7%Fe	BCC-Ta
"3" in Fig. 5(c)	47%Ta53%Fe	Laves-TaFe[c]
"4" in Fig. 5(c)	4%Ta96%Fe	BCC-Fe
"1" in Fig. 6(b)	99%Ta1%Fe	BCC-Ta
"2" in Fig. 6(b)	81Ta19%Fe	MU-TaFe
"1" in Fig. 7(a)	98%Ta2%Fe	BCC-Ta
"2" in Fig. 7(a)	54%Ta46%Fe	Laves-TaFe
"3" in Fig. 7(a)	1%Ta99%Fe	BCC-Fe

[a]BCC was body-centered cubic phase;

[b]MU was a topologically closely-packed (TCP) phase, e.g., A_7B_6;

[c]Laves was a AB_2-type TCP phase

temperature in this zone was dynamically changing and was difficult to detect experimentally. However, based on the fact that the solid diffusion took place here, it was reasonable to use all solid phases in both Ta core and Fe shell parts in the model. As the Fe-Ta alloy's melting point was about 1700-2000 K (see Ta-Fe phase diagram), the diffusion temperature was set at this range (1900 K was used). The result showed that the elemental interdiffusion between the Ta core (BCC phase) and the Fe shell (BCC phase) promoted the formation of phases such as MU or Laves. The chemical composition of the Laves phase, according to the Ta-Fe phase diagram, was about 60%Ta40%Fe, which basically agreed with the EDS measurement ("2" 54%Ta46%Fe in Fig. 7a).

Based on the experimental results above, a schematic drawing of the microstructure development in the Ta layer made by laser cladding technique on the Fe substrate is given in Fig. 8. In the laser beam heating zones, Ta can be fully molten (FM zone) and then to form typical dendritic structure containing BCC-Ta dendrite and MU-TaFe inter-dendrite during solidification. As Fe upward diffusion occurred at the same time, the fraction of the Ta dendrites decreased closer to the Fe substrate. Beside the FM zone directly under the laser beam, PM zones were formed
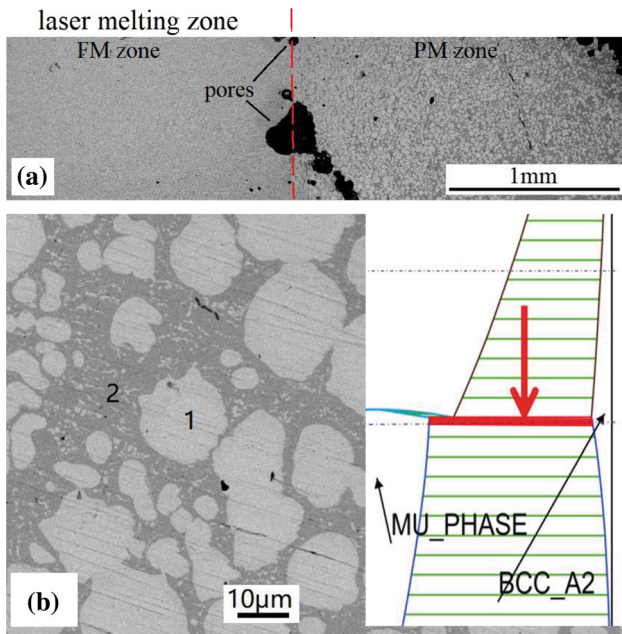
Fig. 6 (a) Microstructure showing fully molten (FM) zone and partially molten (PM) zone, (b) microstructure in PM zone and its corresponding phase diagram

where Ta powders were also piled up and partially molten. At the edge corners of the PM zones, solid diffusion would also occur between Ta powders and the surrounded Fe to form core–shell structure. Obviously, the laser melting of Ta was strongly affected by the upward diffusion of Fe. Therefore, it is very important to take the diffusion effect of the substrate elements into account when cladding a refractory element layer on a low melting-point substrate.

Laser-Cladded Ta and Plasma-Sprayed Ta on Tungsten Substrates

To achieve a purer Ta layer for high-quality rotating sputtering targets, the diffusion of the substrate elements should be minimized. So, we changed the substrate from iron to tungsten which had a higher melting point than Ta. Two technical methods were tried, i.e., laser cladding and plasma spraying. Figure 9 compares the microstructure of the cladded and sprayed Ta layers. As discussed above, a Ta-Fe dendritic structure was formed if using iron as the substrate (Fig. 9a). But if using W as the substrate, as shown in Fig. 9(b), no dendritic structure was formed and the Ta matrix was much purer according to EDS measurement. The W content detected in the Ta layer was
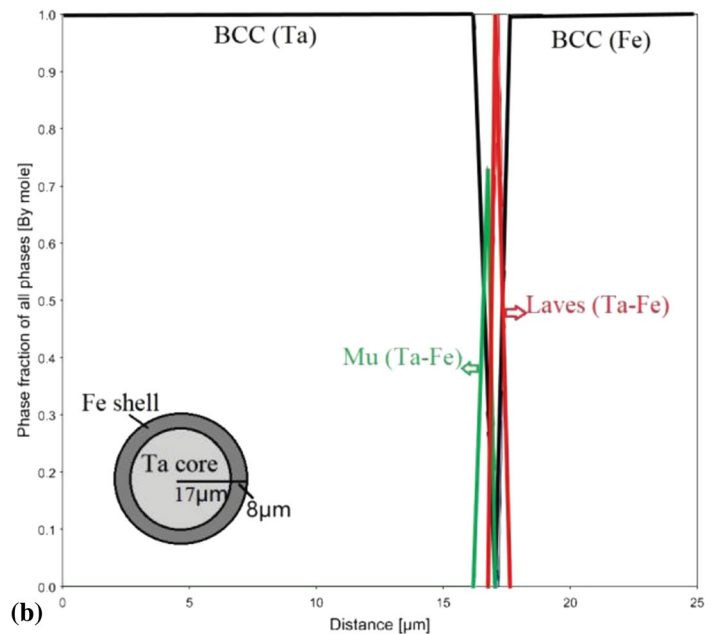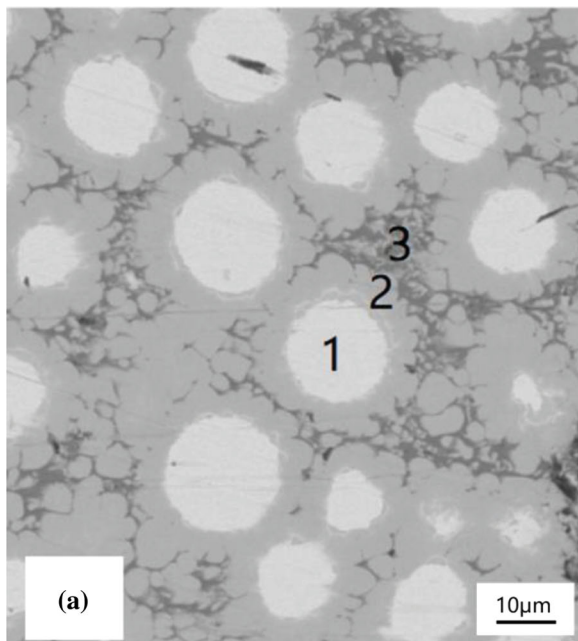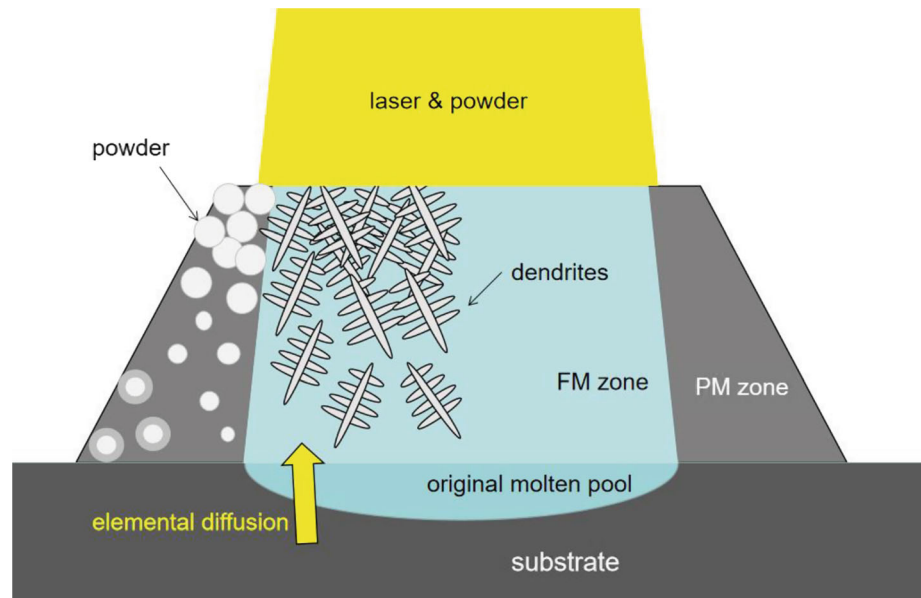

Fig. 7 (a) Solid diffusion microstructure at the corner of PM zones, (b) calculated microstructure distribution in Ta-Fe core–shell structure (1900 K result)

Fig. 8 Schematic drawing of microstructure development in Ta-cladded layer on Fe substrate

lower than 0.5% which was actually under the detection error of EDS technique. Some Ta-oxides were also formed in the Ta matrix which was inevitable made in the air environment. The plasma-sprayed Ta coating (Fig. 9c) shows typical splat structures. An EDS measurement also showed a highly pure Ta matrix with little substrate element W detected. According to the image analyzing on porosity, both the cladded Ta layer and the plasma-sprayed Ta coating on the W substrates were dense (porosity less than 2%). As the spraying technology did not require a hot substrate, it is possible to make pure Ta coatings on a lower-melting-point substrate. However, the efficiency of the plasma spray technique was much lower than that of the laser cladding.

Figure 10 gives a schematic drawing of the mechanism of the microstructure development in three different cases, i.e., laser cladding on Fe substrate, laser cladding on W substrate and plasma spray on W substrate. When using a low-melting-point substrate in laser cladding process (Fig. 10a), the upward diffusion of the substrate elements was strong, and some dendritic microstructure could be formed. When using a high-melting-point substrate (Fig. 10c), the molten pool was much smaller and the diffusion of the substrate elements can be minimized. So, a purer Ta layer can be produced by the laser cladding technique when choosing a suitable substrate. Plasma spray technology is another candidate approach to make pure and

dense Ta coatings which had a typical splat-to-splat structure. Taken together, laser cladding was a better selection to make thick and high-quality coatings for rotating sputtering targets with using refractory elemental substrates.

Conclusions

(1) In the case of laser-cladded Ta on Fe substrate, the microstructure of the Ta layer was much affected by the upward diffusion of Fe from the substrate. In the fully molten zone, typical dendritic structure was formed containing BCC-Ta dendrite and MU-TaFe inter-dendrite. While in the partially molten zone, spherical Ta particle morphology was kept. The results indicates that when the cladding layer element had much higher melting point than the substrate element, the effect of the upward diffusion of the substrate elements on the melting and solidification processes of the refractory elements must be taken into account.

(2) To achieve high-quality Ta layers or coatings by minimizing the effect of the upward diffusion of substrate elements, high-melting-point tungsten substrates were used in the laser cladding process. The results showed that the W content (substrate
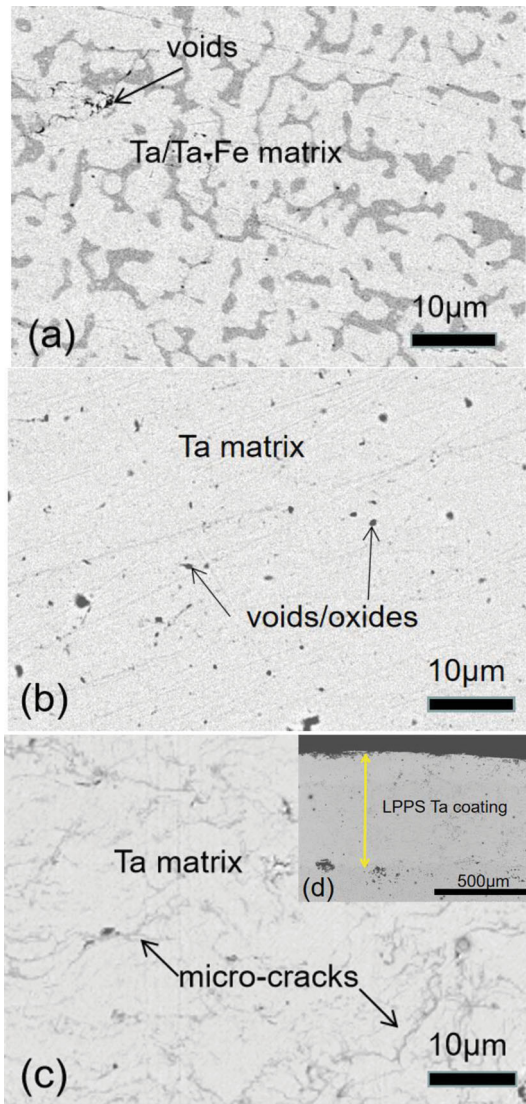
Fig. 9 Microstructure of Ta layers/coatings: (a) laser-cladded on iron substrate, (b) laser-cladded on W substrate, (c) and (d) plasma-sprayed on W substrate
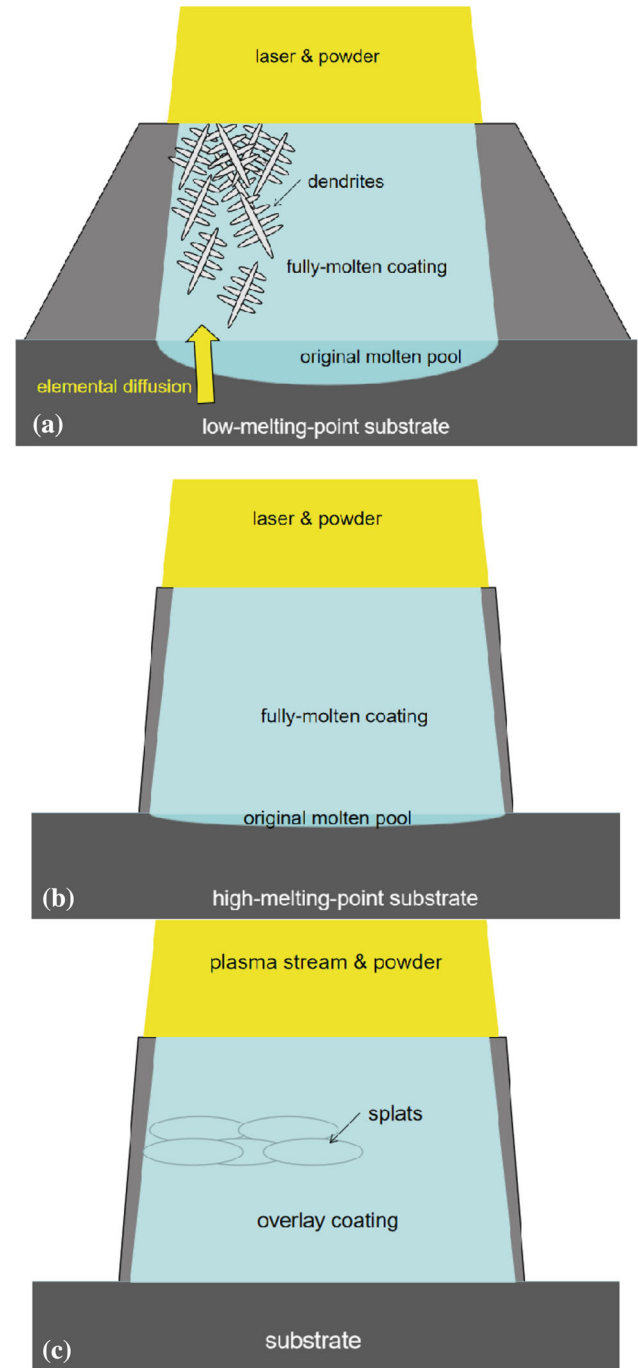

Fig. 10 Schematic drawing of microstructure development in (a) laser-cladded Ta coating on low-melting-point substrate, (b) laser-cladded Ta coating on high-melting-point substrate, (c) plasma-sprayed Ta coating

element) in the Ta layer was very limited indicating a significant improvement of the purity. Laser cladding technique was considered to be a good approach to efficiently make thick and high-quality coatings with using refractory elemental substrates.

References

1. C. Rowe, The Use of Tantalum in the Process Industry, *J. Miner. Met. Mater. Soc.*, 1997, **49**(1), p 26-28.

2. R. Wauthle, V. Johan et al., Additively Manufactured Porous Tantalum Implants, *Acta Biomater.*, 2015, **14**, p 217-225.

3. C. Bauche-Arnoult, J. Bauche et al., Dielectronic Recombination Process in Laser-Produced Tantalum Plasmas, *Phys. Rev. A*, 1989, **39**(3), p 1053-1065.

4. R. Vert, R. Pontone, M.I. Boulos, Induction Plasma Technology Applied to Powder Spheroidization, Densification And Recycling, in *World PM2016 Congress*, (Hamburg(DE), 2016).

5. S. Uesaka, Induction Plasma Spheroidization of Molybdenum Powder, in *18th ISPC*, 2007.

6. C. Sungail and A.D. Abid, Additive Manufacturing of Tantalum – A Study of Chemical and Physical Properties of Printed Tantalum, *Met. Powder Report*, 2020, **75**(1), p 28-33.

7. R. Gavrilova and V. Hadzhiyski, Synthesis and Spheroidization of Disperse High-Melting (refractory) Powders in Plasma Discharge, *Ann. Dunarea de Jos Univ. Galati Fascicle IX Metall. Mater. Sci.*, 2011, **34**(3), p 66-70.

8. Q. Qin, F. Yang et al., Spheroidization of Tantalum Powder by Radio Frequency Inductively Coupled Plasma Processing, *Adv. Powder Technol.*, 2019, **30**(8), p 1709-1714.

9. M. Zhong, W. Liu et al., Formation of WC/Ni Hard Alloy Coating by Laser Cladding of W/C/Ni Pure Element Powder Blend, *Int. J. Refractory Met. Hard Mater.*, 2006, **24**(6), p 453-460.

10. W. Zhang, Research of Microstructure and Hardness of Co55 and W Coating Made by Laser Cladding, *Adv. Mater. Res.*, 2015, **1120–1121**, p 694-697.

11. R.L. Sun, D.Z. Yang et al., Laser Cladding of Ti-6Al-4V Alloy with TiC and TiC+NiCrBSi Powders, *Surf. Coat. Technol.*, 2001, **135**(2–3), p 307-312.

12. T.A.M. Haemers, D.G. Rickerby et al., Laser Cladding of Stainless Steel with Hastelloy, *Adv. Eng. Mater.*, 2001, **3**(4), p 242-245.

13. R. Yang, D. Ge et al., Study on Tantalum Coating on Titanium Alloy Surface by Laser Cladding, in *Proceedings of 21st International Conference on Composite Materials*, (Xi'an , 2021).

14. J.P. Kusinski, J. Przybylowicz, and A. Woldan, Laser Alloying and Cladding of Metallic Substrates, *Int. Soc. Opt. Photon.*, 2000, **4238**, p 101-114.